

Research Article

Experimental Study on Mechanical Properties of Gas Storage Sandstone under Water Content

Sinan Zhu ^{1,2,3}, Junchang Sun ³, Yingjie Wu ⁴, Baoyun Zhao ⁴, Li Zhang ⁴,
Xin Zhang ⁴ and Bingyuan Wang ⁴

¹University of Chinese Academy of Sciences, Beijing, China

²Institute of Porous Flow & Fluid Mechanics, Chinese Academy of Sciences, Langfang, China

³PetroChina Research Institute of Petroleum Exploration & Development, Beijing, China

⁴School of Civil Engineering and Architecture, Chongqing University of Science and Technology, Chongqing 401331, China

Correspondence should be addressed to Junchang Sun; sunjunchang10@petrochina.com.cn and Baoyun Zhao; baoyun666@cqust.edu.cn

Received 1 July 2021; Accepted 29 August 2021; Published 22 September 2021

Academic Editor: Giosuè Boscato

Copyright © 2021 Sinan Zhu et al. This is an open access article distributed under the Creative Commons Attribution License, which permits unrestricted use, distribution, and reproduction in any medium, provided the original work is properly cited.

In order to investigate the influence of water content on the damage and degradation characteristics of Hutubi sandstone, different saturation experiments and laboratory mechanical experiments were carried out on Hutubi sandstone. The experimental results show that under uniaxial and triaxial conditions, with the increase in water content, the axial, lateral, and volume deformations gradually increase, and the deformation shows obvious dilatancy characteristics. The deviator stress and elasticity modulus of the sandstone decreased exponentially with the increasing water content. Confining pressure has a significant effect on the strength improvement of sandstone under the constant water content. Based on lognormal distribution, the damage constitutive model of sandstone which can reflect both uniaxial and triaxial condition with different water contents was proposed. The theoretical curves were compared with the experimental curves, and it was found that the theoretical curves and the experimental curves have similar changing trends. It shows the rationality of the statistical damage constitutive model.

1. Introduction

The evolution law of rock mechanical properties is of an important guiding significance for underground gas storages built. It is well known that the evolution law of rock mechanical properties is not only affected by the constituent materials and internal original cracks [1]. It is also affected by environmental factors, and the influence of water content is particularly prominent. The degrading effect of water on rocks causes many rocks engineering hazards. So, it is of great significance to explore the degradation mechanism of water on rocks.

The influence of water content on rock mechanical properties has been extensively studied. These are mainly concerned with the influence of different saturated conditions on the properties of rocks. Vasarhelyi and Van [2] explored the influence trend of the moisture on the rock

strength and found that the water sensitivity of the sandstone largely depends on the effective porosity of the rock. Hawkins and McConnell [3] studied the evolution of the sandstone strength and the water content and found that most strength loss of the sandstone occurred in the condition of low water content. Guha Roy et al. [4] investigated the mechanical parameters of three sandstones affected by the saturation time and found that the relevant mechanical parameters of the rock were decreased with the increase in saturation. Liu et al. [5] described the variation between sandstone immersion time and water distribution and established the equation relationship between uniaxial compressive strength and water distribution. Fu et al. used nuclear magnetic resonance technology to visualize and quantify the penetration path and distribution of water in sandstone. Furthermore, the influence of water on the mechanical properties of sandstone was also evaluated [6].

Based on the indoor experiment, the damage theory of rock was rapidly developed. Rafiei Renani and Martin [7] carried out laboratory mechanical experiments on granite and limestone, and based on the experimental results, a nonlinear constitutive model was proposed to express the relationship between cohesion and internal friction. Kachanov et al. [8] proposed the concept of continuity (φ) to reflect the deterioration mechanism of the rock. Combined with the results of a large number of indoor uniaxial compression tests and damage mechanics theory, a constitutive model of rock damage under water weakening action is established [9]. Based on the three-dimensional numerical simulation method and damage theory, a variety of models for describing the evolution of rock failure and damage have been established [10–12]. The energy dissipated under the wet-dry cycle can reflect the energy mechanism of rock damage, and the internal structure of the rock produces irreversible damage under the action of the wet-dry cycle [13].

In the past few years, many researchers have carried out different saturated experiments on different types of rocks, exploring the differences in the impact of water weakening on different rock types. These are mainly concerned with evolving law of physical and mechanical parameters and obtained some achievements. However, the research studies on the impact of water weakening on rock damage under different loads are still limited. Based on the uniqueness of the sandstone in Hutubi gas storage, it is essential to investigate the evolution of the mechanical properties with different water contents and look for a suitable damage constitutive model. In this paper, the surrounding rock of Hutubi gas storage carried out the uniaxial and triaxial compression tests to analyze the influence of water content on its mechanical properties. Finally, a rock damage model for water weakening effect was established and validated by experimental data.

2. Experimental Procedures

A series of uniaxial and triaxial tests on sandstone samples with different water contents were carried out in the laboratory. The following sections describe the experimental procedure in detail.

2.1. Rock Specimen Preparation. The original sandstone specimens for the tests were taken from a deep underground gas well of Hutubi gas storage which is a type of sedimentary rock, and the depth of specimens is around 3585 m. The average unit mass of the nature rock is about 2260 kg/m³. All specimens were polished into standard cylindrical samples according to ISRM [14].

2.2. Determination of Water Content. According to the method suggested by Siegesmund and Snethlage [15], the specimen was tested for water content after each immersion treatment. The main steps of specimen preparation with different water contents are as follows: (1) the rock specimen is put into the drying box to dry for 48 hours, and it is taken

out for weighing; (2) then, the specimen is put into the saturated container for water content treatment under the natural state; and (3) the rock specimen is weighed at certain intervals, and its saturation is calculated. When the specimen reaches the specified water content, it is taken out for testing.

2.3. Testing Apparatus and Procedure. As shown in Figure 1, all tests are carried out on the TFD-2000 electro-hydraulic servo rock triaxial testing machine. The characteristic of the electro-hydraulic servo rock pressure system is that the whole process is computer controlled and data are automatically collected. While ensuring the accuracy of the data, it also makes the operation easier. Axial pressure loading is controlled by the servo oil source, and the control system will automatically correct the deviation with the target value until it is reached. The maximum axial pressure can reach 2000 kN, and the error is controlled within 10 N. The confining pressure is loaded by filling the pressure chamber with hydraulic oil. Through servo motor control, the maximum confining pressure can reach 100 MPa, and the error is controlled within 0.01 MPa. The function and accuracy of the testing machine can support the smooth progress of this research.

The testing procedure of this study included two series of testing: (1) conventional triaxial compression tests in which the loading is carried out in accordance with the prescribed operating procedures until the specimen is broken and (2) the uniaxial and triaxial compression tests in which the specimens with different water contents are considered. The physical parameters and experimental conditions of the specimens are shown in Table 1.

3. Results and Analysis

3.1. Testing Results of the Gas Storage Sandstone with Different Water Contents

3.1.1. Stress and Strain Analysis of Sandstone with Different Water Contents under Uniaxial Compressive Condition. Figure 2 shows the stress-strain curve of sandstone with different water contents under uniaxial compression. It can be easily obtained that the uniaxial compressive strength gradually decreases with the increase in water content. From dry state to water content of 2.31% and 3.09%, the uniaxial compressive strength of rock specimens decreases by 22.42% and 29.89%, respectively. It can be also obtained that there are generally four stages in the compression process of sandstone, namely, the compaction stage of the microcracks, the elastic deformation stage, the plastic yield deformation stage, and the failure stage after the deviator stress, as shown Figure 3. It can be seen from Figure 2 that there is little difference in the microcrack compaction stage, indicating that the water content has low relativity to the rock specimen in this stage. However, in the elastic deformation stage, the slope of stress-strain curve decreases with the increase in water content significantly. This indicates that the elastic modulus of sandstone has an obvious weakening trend.



FIGURE 1: Rock mechanics experimental system of TFD-2000.

TABLE 1: The specimen basic information and testing procedure.

No.	Diameter (mm)	Length (mm)	Density (g/cm ³)	Confining pressure (MPa)	Water content (%)
3-32-14-2	25.30	52.00	2.23	10	2.31
3-32-14-3	25.30	51.20	2.22	20	2.31
3-32-14-5	25.20	51.10	2.28	30	2.31
3-32-14-7	25.30	52.30	2.22	45	2.31
3-32-14-8	25.20	52.50	2.23	45	3.09
5-21-23-6	24.92	50.58	2.13	45	0
5-10-23-10	25.07	50.80	2.05	45	1.54
12-36-15-6	25.20	50.80	2.07	0	0
4-1-29-10	24.78	51.54	2.08	0	1.54
12-36-15-7	25.20	51.00	2.05	0	2.31
12-36-15-8	25.00	51.10	2.09	0	3.09

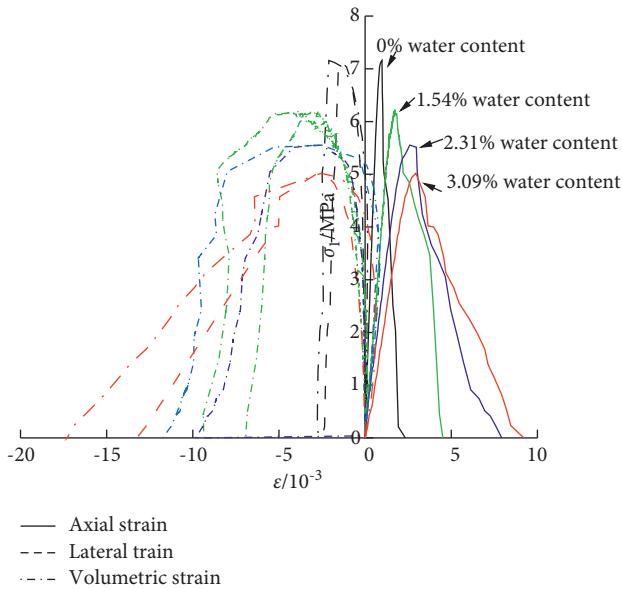


FIGURE 2: Total stress-strain curves with different water contents under uniaxial compression.

3.1.2. Analysis of Sandstone with Different Water Contents under Triaxial Compressive Condition. Figure 4 shows the total stress-strain curves of Hutubi sandstone under triaxial compression with different water contents. It can be seen from Figure 4 that the triaxial compressive strength of Hutubi sandstone decreases with the increase in water content, and the deviator stress at 2.31% water content is 14.65% higher than that at 3.09% water content. Similarly, if we divide the

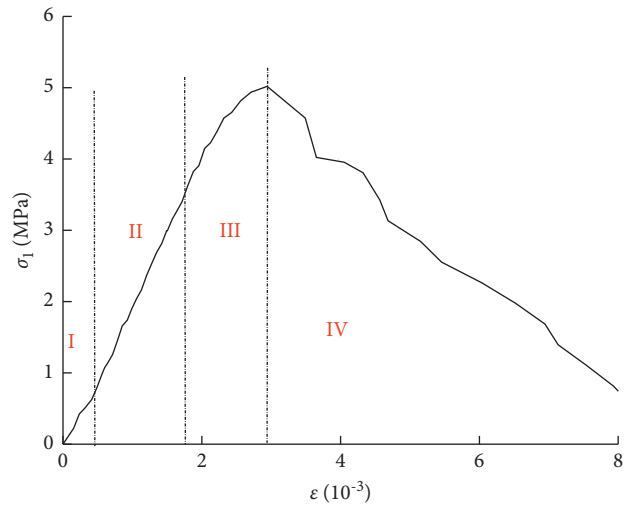


FIGURE 3: The stage of uniaxial compression curve under the water content of 3.8%.

experiment curve of triaxial compression into three stages of the elastic deformation stage, the plastic yield deformation stage, and the postpeak strength stage, it can be obtained that the experimental curves of the specimens with different water contents in the compaction stage and the elastic stage basically coincide. After entering the elastic stage, the water content has a significant weakening effect on the elastic modulus. The primary cracks in the rock are treated with water, which is the main reason for the softening of sandstone. In the yield stage, the specimens with higher water content can lead to the yield stage earlier. In the postpeak strength stage, the strength of the

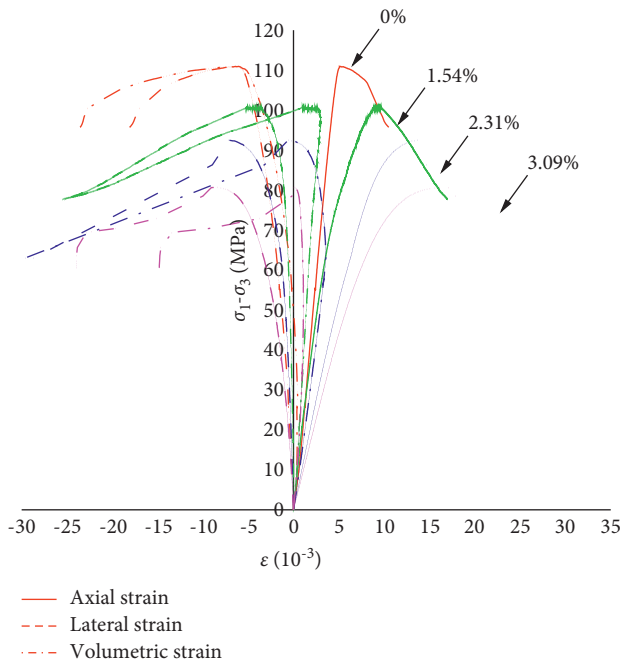


FIGURE 4: Total stress-strain curve under the confining pressure of 45 MPa with different water contents.

specimens tends to be dropped much more slowly and the damage of the specimen gradually presents plastic failure characteristics in higher water content condition.

3.1.3. Stress and Strain Analysis of Sandstone with Constant Water Content under Triaxial Compressive Condition. In this section, the triaxial compressive tests with constant water content (2.31%) were conducted to comparative analysis with different water contents. In Figure 5, the experiment curve of sandstone with 2.31% under different confining pressures is shown. It is found that the deviatoric stress of sandstone at 20 MPa, 30 MPa, and 45 MPa is increased by 75.14%, 151.44%, and 233.74%, respectively, compared with the confining pressures of 10 MPa. It shows that the confining pressure significantly improves the bearing capacity of sandstone. Similarly, the experiment curve of sandstone is divided into linear elastic stage, yield stage, and failure stage. At the initial stage of loading, the specimen directly enters the stage of linear elastic, and the stress rises steadily with the increase in strain showing obvious elastic characteristics while the slope of linear elastic stage decreased gradually. The antidestructive ability of sandstone is improved by the increase in confining pressure, which is manifested in that the specimen needs higher stress from yield to failure, and the failure form gradually changes to plastic failure. Finally, the specimen is broken, and the curve shows a downward trend.

3.2. Analysis of the Gas Storage Sandstone Mechanical Properties with Different Water Contents

3.2.1. Mechanical Property of Sandstone in Triaxial Condition. As shown in Figure 6, under different confining pressures, sandstone with 2.31% water content still follows the

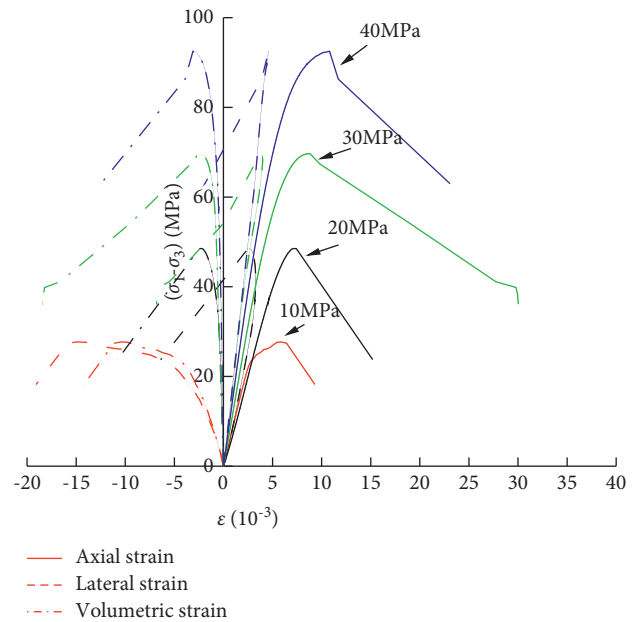


FIGURE 5: Total stress-strain curves with 2.31% water content in triaxial condition.

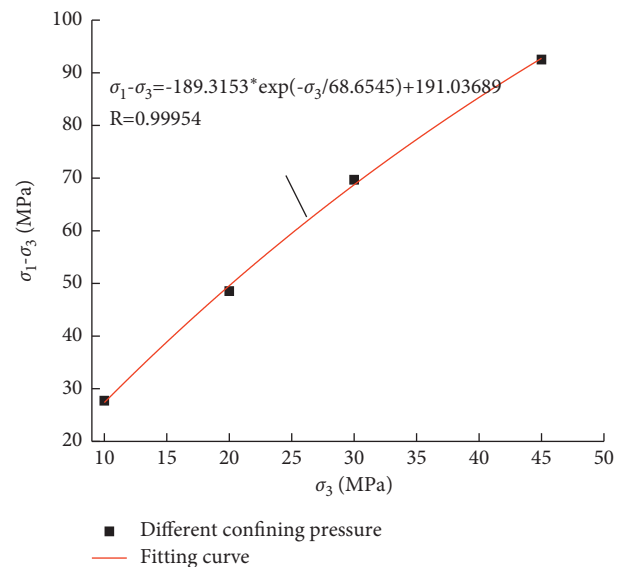


FIGURE 6: The relationship between deviatoric stress and confining pressures with the water content of 2.31%.

law of the deviatoric stress increases with increase in the confining pressure. The deviator stress and the confining pressure show an exponential growth relationship, the growth trend of the deviator stress gradually decreases, and the confining pressure effect gradually decreases. The deviatoric stress, axial strain, and lateral strain of the specimen are all positively related to the confining pressure.

Table 2 shows the strength and mechanical indexes of sandstone with a water content of 2.31% under triaxial conditions. Figure 7 presents the changing trend of the elastic modulus under the changing state of the confining pressure. It was found that the elastic modulus, deformation modulus,

TABLE 2: Mechanical parameters of sandstone under different confining pressures.

σ_3 (MPa)	Water content (%)	E (GPa)	$\varepsilon_{\max}/10^{-3}$
0	2.31	2.61	2.59
10	2.31	8.79	5.85
20	2.31	8.17	7.16
30	2.31	11.53	8.81
45	2.31	14.10	10.81

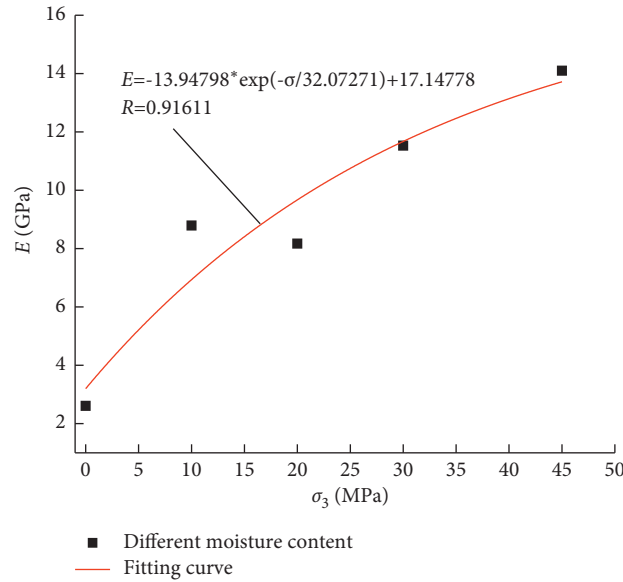


FIGURE 7: The change trend of the elastic modulus and the confining pressures with the water content of 2.31%.

and peak strain of sandstone are positively correlated with confining pressure. When the confining pressure is 0–10 MPa, the increase rates of elastic modulus, deformation modulus, and peak strain are 2.37 times, 2.34 times, and 1.26 times, respectively. From the confining pressure of 10 MPa to 45 MPa, elastic modulus, deformation modulus, and peak strain increase by 60.4%, 72.1%, and 84.8%, respectively.

3.2.2. Analysis of Mechanical Property of Sandstone with Different Water Contents. Figure 8 presents the relationship between the elastic modulus and water content e under uniaxial and triaxial condition. The elastic modulus of sandstone is taken according to the slope of the elastic phase of its stress-strain curve [16]. As shown in Figure 8, the elastic modulus decreases faster when the water content is low and decreases slowly when the water content is high, showing an exponential relationship. Under the uniaxial condition, it was found that the elastic modulus of dried specimen is 2.83 GPa, and the elastic modulus of the specimen with 1.54% water content is 2.61 GPa, the elastic modulus has decreased around 50.66%, and the elastic modulus of the sandstone specimens with the water content of 2.03% and 3.09% has decreased around 73.24% and 75.99%, respectively. Compared with the dry condition, the elastic modulus of the sandstone specimens with the water content of 1.54%, 2.03%, and 3.09% under triaxial condition has decreased around 43.42%, 52.04%, and

55.82%, respectively. The reason is that the loss of water is accompanied by some mineral particles. This causes the porosity of the rock specimens to increase and accelerates the deterioration of the sandstone.

4. Discussion on Damage Constitutive Models with Different Water Contents

4.1. The Establishment of Damage Constitutive Model.

Rock is a natural industrial raw material, but it is usually accompanied by a large number of original cracks, pores, and weak structural surfaces. These initial defects are also typical manifestations and important reasons of rock damaged [17]. The statistics damage constitutive model [18] is one of the widely used damage constitutive models in rock engineering, which regarded rock as a heterogeneous failure process of partial microrock units, and the function of which could be expressed as follows:

$$P_{(\varepsilon)} = \frac{a}{b} \left(\frac{\varepsilon}{b} \right)^{a-1} \exp \left[- \left(\frac{\varepsilon}{b} \right)^a \right], \quad (1)$$

where ε is the rock strain and a and b are the physical and mechanical property parameters of rock.

The damage variable of the rock can be determined by the ratio of the number of damaged microrock units to the total number of microrock units, which can be expressed as follows [19]:

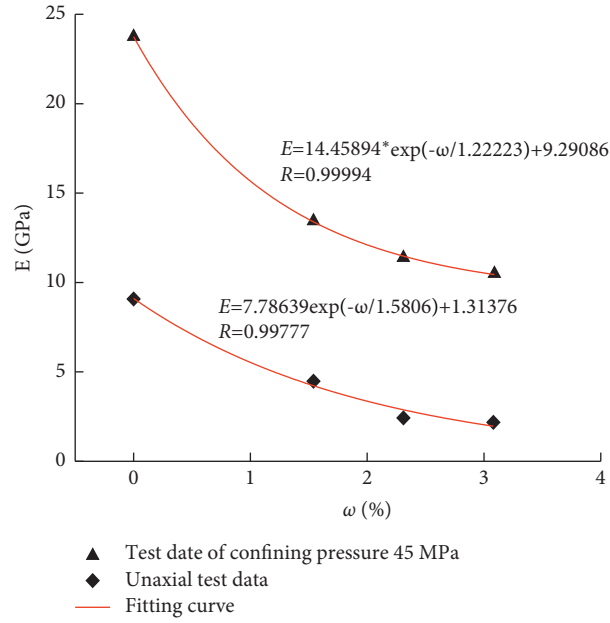


FIGURE 8: Relationship between elastic modulus and water content.

$$D_l = \frac{N_\varepsilon}{N} = 1 - \exp\left(-\left(\frac{\varepsilon}{b}\right)^a\right), \quad (2)$$

where N is the total number of microrock units.

According to the relationship between elastic modulus and water content, as shown in Figure 7, we assume that the damage induced by water content can be expressed as follows:

$$D_w = 1 - \exp\left(\frac{w}{d}\right), \quad (3)$$

where w is the water content and d is the physical and mechanical property parameters of rock.

When the two are coupled, the damage state of the rock after the action of water content is used as an indicator [20]. After the sandstone is loaded in the experiment until it reaches failure, its total damage variable (D) can be considered to be composed of two parts, namely, the moisture content and the impact caused by the loading, and the following equation can be obtained:

$$D = 1 - (1 - D_l)(1 - D_w) = D_l + D_w - D_l D_w. \quad (4)$$

Based on the principle of equivalent strain, the stress-damage relation of the sandstone under uniaxial condition could be shown as follows:

$$\sigma = E_0 (1 - D)\varepsilon. \quad (5)$$

According to the Lemaitre equivalent strain principle [21] and the generalized Hooke's law, the constitutive equation of rock under triaxial compression can be described as follows:

$$\sigma_1 = E_0 \varepsilon_1 (1 - D) + 2\mu\sigma_3, \quad (6)$$

where μ is Poisson's ratio.

4.2. Damage Evolution Analysis. Take the uniaxial compressive tests result with different water contents as example, the damage evolution can be calculated by equation (4) combined with equations (2) and (3). Figure 9 presents the damage evolution of sandstones with different water contents under uniaxial compression tests. It was found that the accumulation rate of damage in the elastic stage is slow, and the accumulation rate of damage obviously shows an upward inflection point when the curve enters the yield stage. In the postpeak strain softening stage, the damage keeps accumulating at a high speed, and the strain value is close to the peak strain when the specimen is completely broken.

As shown in Figure 10, it is the evolution curve of the total damage variable with different water contents in the uniaxial state. From Figure 9, it is also shown that water content is higher, the smaller the damage variable under the same strain. In the state of high-water content, the damage develops slowly with the accumulation of strains. It shows that the increase in water content will affect the failure characteristics of rock, and its failure characteristics will change from brittleness to toughness.

4.3. Verification of Damage Constitutive Model. The comparison between the experimental results and the calculation results of equation (5) under different water contents shows that the proposed damage model fits well with the experimental data, as shown in Figure 11. It shows that the experimental curves of sandstone specimens affected by the water content and uniaxial loading can better reflected by equation (5). Meanwhile, the calculated results by using equation (6) were also used in contrastive analysis of the experimental results under the confining pressure of 45 MPa with different water contents and found that the calculated curves can well agree with the experimental curves, as shown in Figure 12. Therefore,

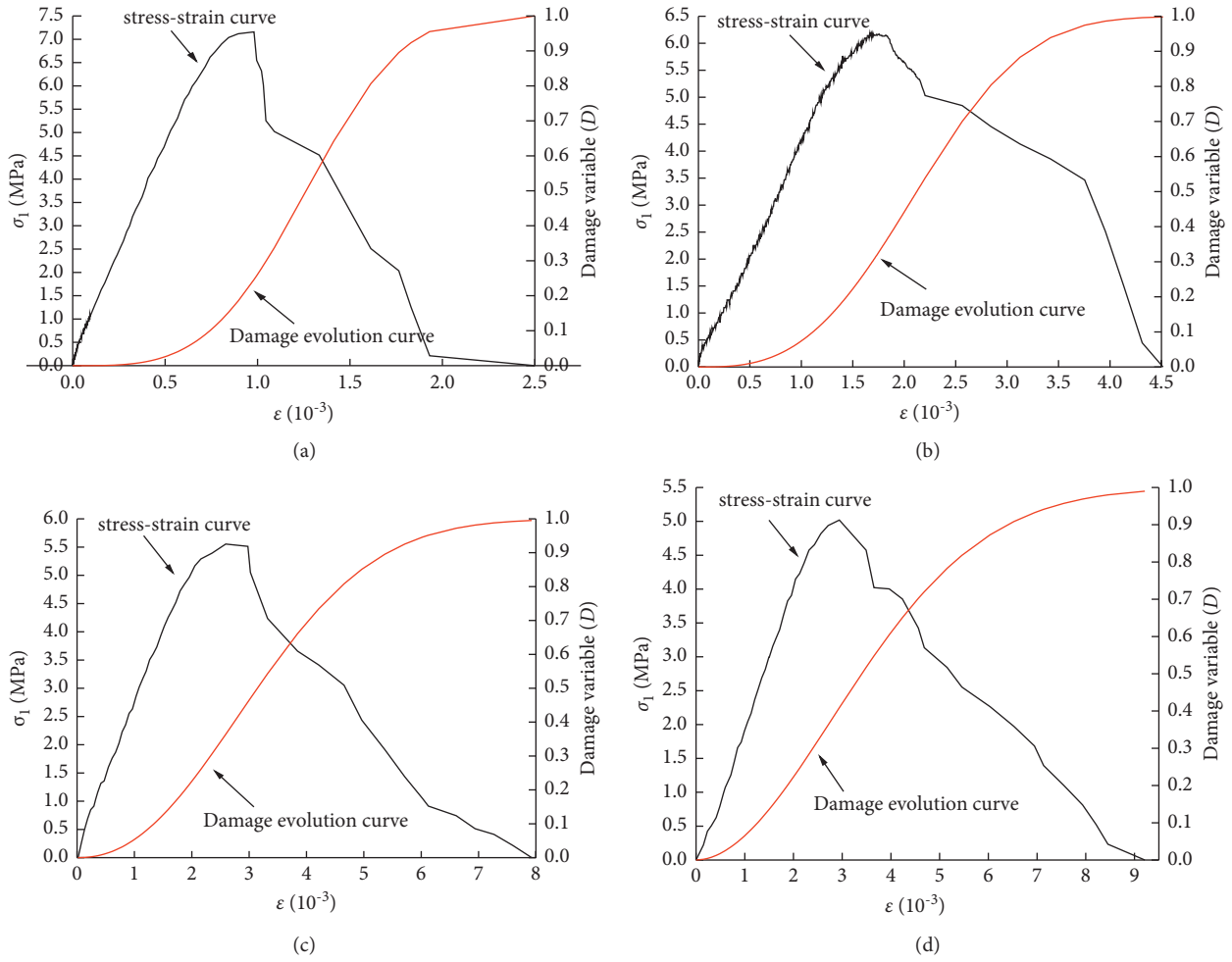


FIGURE 9: Damage evolution curves of uniaxial compression with different water contents: (a) 0% water content; (b) 1.5% water content; (c) 2.7% water content; (d) 3.09% water content.

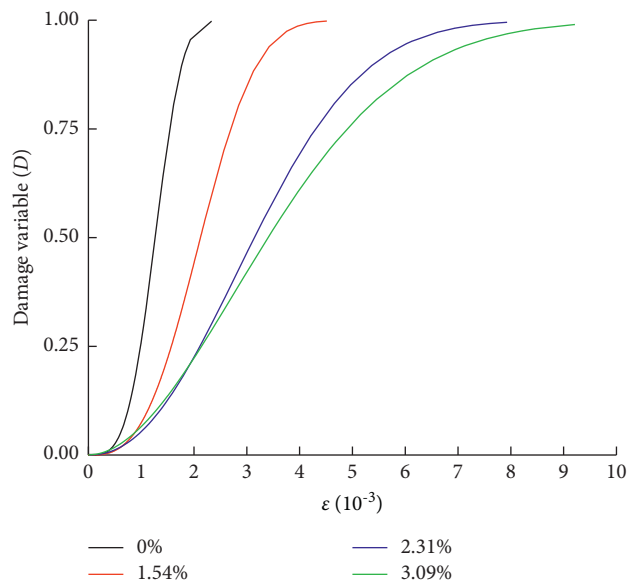


FIGURE 10: Damage evolution curves of uniaxial compression with different water contents.

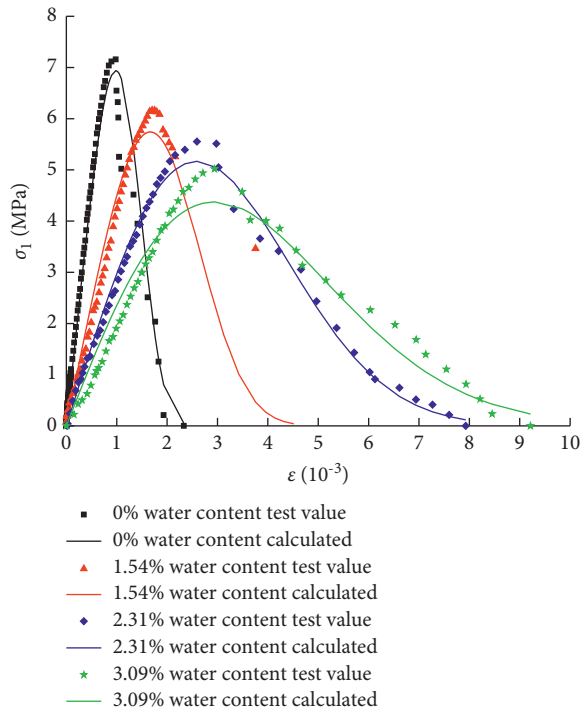


FIGURE 11: Theoretical and experimental curves under different water contents.

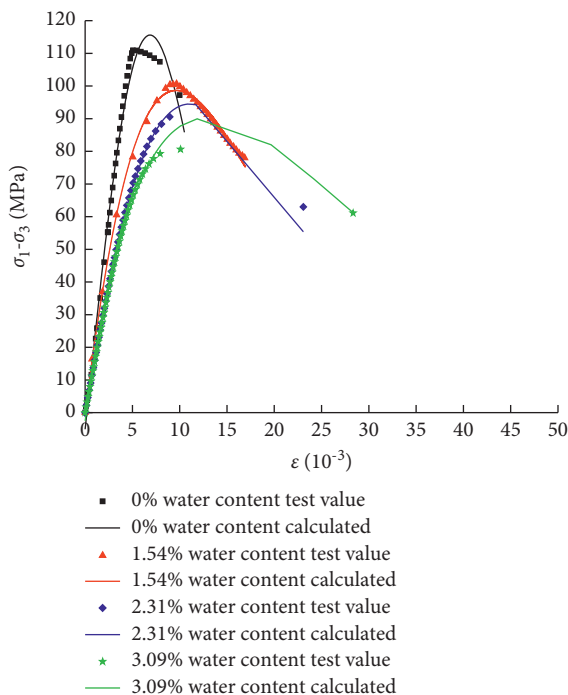


FIGURE 12: Theoretical and experimental curves under different water contents in 45 MPa.

the proposed model can be used to better predict the effect of different water contents and also has a certain reference value for actual engineering.

5. Conclusions

In this paper, sandstone collected from Hutubi gas storage was chosen to report the mechanical properties with different water contents, and the damage involution of which with different water contents was analyzed in detail. The following conclusions can be drawn.

The exponential function relationship is used to describe the deviatoric stress and elastic modulus of sandstone decreasing with water content. The loss of pore water causes the loss of mineral particles, and the chemical reaction between mineral particles and pore water is the main reason for this phenomenon. In addition, the appearance of pore water pressure in the experiment also accelerates the degradation rate of sandstone.

Through theoretical derivation, this paper proposed a damage constitutive model of sandstone with different water contents based on lognormal distribution and compared the calculated theoretical curves with the experimental curves. The rationality of the damage constitutive model is proved by the high similarity between the theoretical curve and the experimental curve.

Data Availability

The data used in the tests of this study are included within the article.

Conflicts of Interest

The authors declare that there are no conflicts of interest in this paper.

Acknowledgments

This work was supported by the National Natural Science Foundation of China (No. 41302223), the Natural Science Foundation of Chongqing (Nos. cstc2020jcyj-msxm1078 and cstc2020jcyj-msxmX0558), and the Chongqing University of Science and Technology Graduate Students' Science and Technology Innovation Program (No. YKJCX2020653).

References

- [1] D. M. Gu, H. L. Liu, X. C. Gao, D. Huang, and W. G. Zhang, "Influence of cyclic wetting-drying on the shear strength of limestone with a soft interlayer," *Rock Mechanics and Rock Engineering*, vol. 2021, no. 22, 2021.
- [2] B. Vásárhelyi and P. Ván, "Influence of water content on the strength of rock," *Engineering Geology*, vol. 81, no. 1-2, pp. 70-74, 2006.
- [3] A. B. Hawkins and B. J. McConnell, "Sensitivity of sandstone strength and deformability to changes in moisture content," *The Quarterly Journal of Engineering Geology and Hydrogeology*, vol. 25, no. 2, pp. 115-130, 1992.
- [4] D. Guha Roy, T. N. Singh, J. Kodikara, and R. Das, "Effect of water saturation on the fracture and mechanical properties of

- sedimentary rocks,” *Rock Mechanics and Rock Engineering*, vol. 50, no. 10, pp. 2585–2600, 2017.
- [5] H. Liu, W. Zhu, Y. Yu, T. Xu, R. Li, and X. Liu, “Effect of water imbibition on uniaxial compression strength of sandstone,” *International Journal of Rock Mechanics and Mining Sciences*, vol. 127, no. 2020, p. 104200, 2020.
- [6] T. F. Fu, T. Xu, M. J. Heap, P. G. Meredith, and Y. Nara, “Analysis of capillary water imbibition in sandstone via a combination of nuclear magnetic resonance imaging and numerical dem modeling,” *Engineering Geology*, vol. 285, no. 4, p. 106070, 2021.
- [7] H. Rafei Renani and C. D. Martin, “Cohesion degradation and friction mobilization in brittle failure of rocks,” *International Journal of Rock Mechanics and Mining Sciences*, vol. 106, pp. 1–13, 2018.
- [8] L. M. Kachanov, *The Theory of Creep: Part I*, National Lending Library for Science and Technology, Yorkshire: Boston Spa, 1967.
- [9] K. Bian, J. Liu, W. Zhang, X. Zheng, S. Ni, and Z. Liu, “Mechanical behavior and damage constitutive model of rock subjected to water-weakening effect and uniaxial loading,” *Rock Mechanics and Rock Engineering*, vol. 52, no. 1, pp. 97–106, 2019.
- [10] G. L. Zhou, T. Xu, M. J. Heap et al., “A three-dimensional numerical meso-approach to modeling time-independent deformation and fracturing of brittle rocks,” *Computers and Geotechnics*, vol. 117, Article ID 103274, 2020.
- [11] T.-F. Fu, T. Xu, M. J. Heap, P. G. Meredith, and T. M. Mitchell, “Mesoscopic time-dependent behavior of rocks based on three-dimensional discrete element grain-based model,” *Computers and Geotechnics*, vol. 121, p. 103472, 2020.
- [12] T. Xu, T. F. Fu, M. J. Heap, P. G. Meredith, and P. Baud, “Mesoscopic damage and fracturing of heterogeneous brittle rocks based on three-dimensional polycrystalline discrete element method,” *Rock Mechanics and Rock Engineering*, vol. 53, no. 23, 2020.
- [13] X. Chen, P. He, and Z. Qin, “Strength weakening and energy mechanism of rocks subjected to wet-dry cycles,” *Geotechnical & Geological Engineering*, vol. 37, no. 5, pp. 3915–3923, 2019.
- [14] C. E. Fairhurst and J. A. Hudson, “Draft ISRM suggested method for the complete stress-strain curve for the intact rock in uniaxial compression,” *International Journal of Rock Mechanics & Mining Science & Geomechanics*, vol. 36, no. 3, pp. 281–289, 1999.
- [15] S. Siegesmund and R. Snethlage, *Stone in Architecture: Properties, Durability Environmental & Engineering Geoscience*, Vol. 2014, Springer, Berlin, Germany, 5th edition, 2014.
- [16] Y. F. Wang, H. Su, L. P. Wang, H. Z. Jiao, and Z. Li, “Study on the difference of deformation and strength characteristics of three kinds of sandstone,” *Journal of China Coal Society*, vol. 307, no. 4, pp. 163–170, 2020.
- [17] J. Wang, Z. Song, B. Zhao, X. Liu, J. Liu, and J. Lai, “A study on the mechanical behavior and statistical damage constitutive model of sandstone,” *Arabian Journal for Science and Engineering*, vol. 43, no. 10, pp. 5179–5192, 2018.
- [18] W. Weibull, “A statistical distribution function of wide applicability,” *Journal of Applied Mechanics*, vol. 18, no. 3, pp. 293–297, 1951.
- [19] C. Gao, L. Z. Xie, H. P. Xie et al., “Coupling between the statistical damage model and permeability variation in reservoir sandstone: theoretical analysis and verification,” *Journal of Natural Gas Science and Engineering*, vol. 37, pp. 375–385, 2016.
- [20] H. Zhang and G. Yang, “Research on rock damage model under the coupling action of freeze-thaw and load,” *Chinese Journal of Rock Mechanics and Engineering*, vol. 29, no. 3, pp. 471–476, 1951.
- [21] J. Lemaitre, “How to use damage mechanics,” *Nuclear Engineering and Design*, vol. 80, no. 2, pp. 233–245, 1984.